Dynamics of the Tyrosine Side Chain in *Bombyx mori* and *Samia cynthia ricini* Silk Fibroin Studied by Solid State ^{2}H NMR

Tsunenori Kameda,[†] Youhei Ohkawa,[†] Keiko Yoshizawa,[†] Emi Nakano,[†] Toshifumi Hiraoki,[‡] Anne S. Ulrich,[§] and Tetsuo Asakura*,[†]

Department of Biotechnology, Tokyo University of Agriculture and Technology, Koganei, Tokyo 184-5588, Japan, Department of Applied Physics, Hokkaido University, Sapporo 060-8628, Japan, and Institut für Molekularbiologie, Friedrich-Schiller-Universität Jena, Winzerlaer Strasse 10, 07745 Jena, Germany

Received August 10, 1999

ABSTRACT: Solid-state deuterium NMR (^{2}H NMR) was used to study the dynamics of the tyrosine (Tyr) residue in silk fibroin from *Bombyx mori* (*B. mori*) and *Samia cynthia ricini* (*S. c. ricini*). Specifically deuterated cocoon silk was obtained by feeding silk worms with Tyr, labeled either at the C_β carbon ([3,3-$^2H_2$]Tyr) or at the aromatic ring ([3′,5′-$^2H_2$]Tyr). The ^{2}H NMR spectra of the [3,3-$^2H_2$]Tyr-labeled silk fibroins showed typical rigid powder patterns, indicating that there is essentially no motion about the $C_\alpha-C_\beta$ bond axis, both in *B. mori* and *S. c. ricini*. In contrast, the ^{2}H NMR spectra of the [3′,5′-$^2H_2$]-Tyr-labeled silk fibroins consisted of two dynamic components each: a rigid powder contribution, plus a motionally averaged contribution. Hence, some of the Tyr side chains are mobile at the phenolic ring. This motion was characterized to be a π-flip as is typical of aromatic rings. The corresponding ^{2}H NMR line-shape of the *B. mori* sample could be successfully simulated by attributing 20% of the signal to a motionally averaged component with a fast rate (10^6 Hz) and the remaining 80% to a much slower component ($<10^3$ Hz). Likewise, the simulation of *S. c. ricini* silk fibroin indicated that 60% of the rings are engaged in fast motional averaging (10^7 Hz), while 40% undergo slow motion (10^4 Hz). Thus, the fraction of the fast component is considerably higher for *S. c. ricini* silk fibroin than for *B. mori*, which must be a consequence of their different amino acid sequences. It appears that the side-chain mobility depends on the local packing density around the Tyr residue. We conclude that the Gly-Ala repeats in *B. mori* silk fibroin are relatively tightly packed. In contrast, a large part of the Gly-rich regions in *S. c. ricini* are comparatively loosely packed.

Introduction

Silk fibroin from the domestic silkworm, *Bombyx mori* (*B. mori*), is a fibrous protein which contains 46% glycine (Gly), 29% alanine (Ala), 12% serine (Ser), 4.8% tyrosine (Tyr), and 2.5% valine (Val).[1] Most of its primary structure has been sequenced by Mita et al.,[2] who showed that there are repetitive and nonrepetitive regions. The most abundant repetitive motif has the sequence Gly-Ala-Gly-X-Gly-Ala- (X = Ser or Tyr). We have shown that the Ala and Gly residues of repetitive region are regarded as a candidate for assembly into the β-sheet structure[3] and, more recently, that also the Ser and Tyr residues of the repetitive region occupy a restricted conformational space in the antiparallel β-sheet region.[4] Moreover, we have recently described the structure and dynamics of the Ser side chain,[5] with special attention to the hydrogen-bonding ability of its hydroxyl group. Here, we focus on the dynamics of the Tyr residue, which is also present in the repetitive region as a fraction of about 80% of the total Tyr content. Besides its potential role in hydrogen bonding, Tyr also plays an important role as an active site for covalently immobilizing enzymes onto silk fibers.[6,7]

Samia cynthia ricini (*S. c. ricini*) is a wild silkworm with a rather different amino acid composition and primary sequence from *B. mori*.[8,9] Recently, Yukuhiro et al. have determined the *S. c. ricini* sequence in detail[10] and described its repetitive motif. It consists of a polyalanine stretch of 10−14 Ala, followed by a Gly-rich sequence containing the bulky residues, which is reminiscent of spider dragline silk.[11] The Tyr residues occur mainly in the Gly-rich environment, and approximately 60% of all Tyr in the sequence is present as -Tyr-Gly-Gly-Gly- or -Gly-Gly-Gly-Tyr-.

Solid state ^{2}H NMR is a powerful tool to analyze the local structure and dynamics of selectively deuterium-labeled macromolecules.[12] The spectral line-shape and relaxation behavior are largely determined by the quadrupolar interaction. The observed coupling between the deuterium quadrupole moment and the electric field gradient at the nucleus carries information about the spatial alignment and motional averaging of the labeled segment. ^{2}H NMR line shapes and relaxation times can thus be analyzed in terms of restricted anisotropic motions. Quadrupole echo experiments are generally applicable to the dynamic range of 10^{-7} s $< \tau_c <$ 10^{-3} s,[13] which covers a wide range of different molecular motions, such as backbone dynamics, side-chain flips, or diffusion processes.

The molecular motions of phenyl rings in solids have been extensively investigated by solid-state NMR for amino acids,[14−18] peptides,[19−22] polypeptides,[18,23−29] and proteins.[30−33] Most of the rings are either rigid or undergo π-flips at room temperature, depending on the crystal packing.[14−22] In this paper, the ^{2}H NMR spectra of [3,3-$^2H_2$] and [3′,5′-$^2H_2$] Tyr-labeled fibroins from *B. mori* and *S. c. ricini* are analyzed to obtain further details about the dynamics of this important side chain in the two different types of silk fibers.

[†] Tokyo University of Agriculture and Technology.
[‡] Hokkaido University.
[§] Friedrich-Schiller-Universität Jena.

10.1021/ma991344g CCC: $18.00
Published on Web 11/20/1999

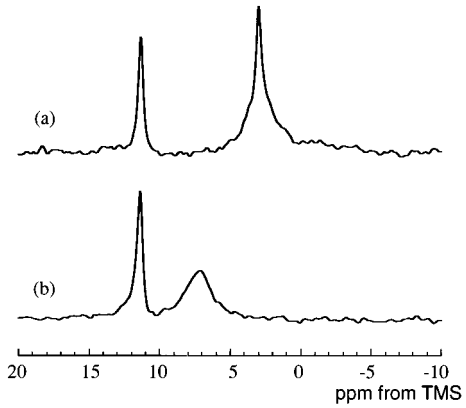

Figure 1. Solution ^{2}H NMR spectra of ^{2}H-labeled *B. mori* silk fibroin dissolved in trifluoroacetic acid (TFA). Samples were obtained from cocoons after rearing the silkworms with an artificial diet containing either [3,3-$^2H_2$]Tyr or [3′,5′-$^2H_2$]Tyr. The chemical shift of the natural abundance TFA CO^{2}H peak is assumed to be 11.3 ppm from TMS.

Materials and Methods

^{2}H-Labeling of Silk Fibroin. Two kinds of ^{2}H-labeled silk fibroins were prepared each from *B. mori* and *S. c. ricini*, by oral administration of an artificial diet containing either [3′,5′-$^2H_2$]Tyr or [3,3-$^2H_2$]Tyr, during the fifth instar larval stage as described earlier.[34] The labeled silk fibroin was obtained from the cocoons and used for NMR after removing another silk protein, silk sericin.[35,36] The ^{13}C NMR spectra of the labeled silk fibroin and the native one were essentially the same. Those results indicate that the labeled silk fibroin has the same structure as the native one.

^{2}H NMR Experiments and Simulations. Spectra of ^{2}H-labeled silk fibers were recorded at 61.25 MHz on a Chemagnetics cmx Infinity 400 NMR spectrometer equipped with a solid state ^{2}H NMR unit. The quadrupole echo sequence ($90°_x - \tau_1 - 90°_y - \tau_2 -$ echo) was used with a 90° pulse length of 3.9 μs and a recycle delay of 0.1, 0.4, or 10 s. Since the echo maximum is not observed exactly at $\tau_1 = \tau_2$ due to finite pulse widths,[37] appropriate left shifts were applied to give effective intervals of $\tau_1 = 50$ and $\tau_2 = 55$ μs. A Lorentzian line broadening of 3 kHz was applied to the spectra prior to Fourier transform. All NMR experiments were performed at room temperature, and the number of accumulations was 20 000. The line-shape simulations were carried out with the program MXQET.[38]

Results and Discussion

^{2}H-Labeling of Silk Fibroin. Parts a and b of Figures 1 show the solution ^{2}H NMR spectra of [3,3-$^2H_2$]Tyr- and [3′,5′-$^2H_2$]Tyr-labeled silk fibroins of *B. mori*, dissolved in TFA.

The natural-abundance CO^{2}H peak of TFA was used as a chemical shift reference and was assumed to be 11.3 ppm from TMS.[39] Its intensity served as a reference to estimate the degree of ^{2}H incorporation into the protein. There is essentially no natural-abundance ^{2}H background from silk fibroin under the experimental conditions used. In Figure 1a only a single sharp peak at around 3 ppm is observed besides the TFA signal, which represents the methylene groups of the [3,3-$^2H_2$]-Tyr side chain. Likewise, the spectrum of Figure 1b shows only one peak at around 7 ppm, which is assigned to the ^{2}H nuclei in the aromatic tyrosine ring. These data show that no metabolic scrambling occurs from the labeled Tyr to other amino acids, at least for the methylene group and aromatic ring.[40] The corresponding [3′,5′-$^2H_2$]Tyr- and [3,3-$^2H_2$]Tyr-labeled silk fibroins of *S. c. ricini* gave ^{2}H NMR spectra similar to those of *B. mori*. The labeling ratios of all samples were high enough for solid-state NMR analysis.

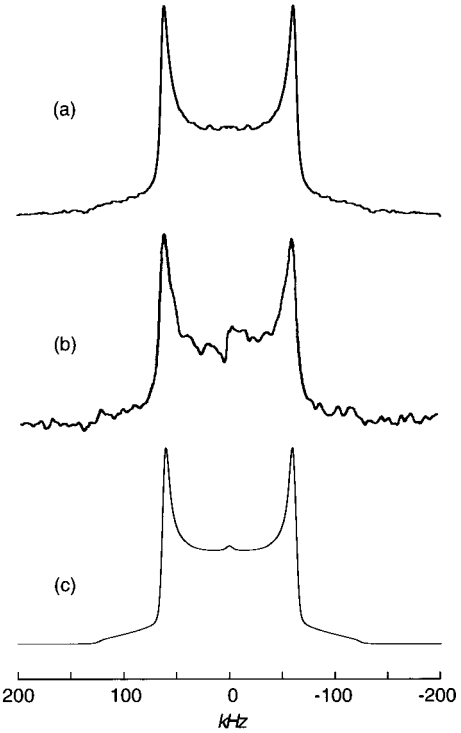

Figure 2. Experimental (a, b) and simulated (c) solid-state ^{2}H NMR spectra. (a) [3,3′-$^2H_2$]Tyr-labeled silk fibroin of *B. mori*; (b) [3,3-$^2H_2$]Tyr-labeled silk fibroin of *S. c. ricini*; (c) spectral simulations based upon a three-site jump model. A 164 kHz quadrupole coupling constant was assumed and a rate constant of 10^3 Hz.

Dynamics of the Tyr Methylene Group. Figure 2 shows the experimental ^{2}H NMR spectra of [3,3-$^2H_2$]-Tyr-labeled *B. mori* (a) and *S. c. ricini* (b) silk fibroin, acquired with a recycle delay of 10 s.

Figure 2c demonstrates that the observed powder line shapes can be successfully simulated with an asymmetry parameter of $\eta = 0.00$ and a quadrupole coupling constant of Qcc = 164 kHz. On the basis of the model of a three-site jump around the $C_\alpha - C_\beta$ bond, a very slow rate constant of 10^3 Hz was used. The agreement between the observed (parts a and b of Figure 2) and simulated (Figure 2c) spectra is good, indicating that the rotation about the $C_\alpha - C_\beta$ bond axis can be considered as essentially static for both *B. mori* and *S. c. ricini* silk fibroin. As will be described below, a large proportion of the Tyr rings undergo fast π-flips with a rate constant of $\geq 10^6$ Hz. Therefore, the predominant side-chain motion of Tyr in silk fibroin is restricted to the phenolic ring.

Dynamics of the Tyr Ring. Figure 3 shows the ^{2}H NMR spectra of [3′,5′-$^2H_2$]Tyr-labeled *B. mori* (a) and *S. c. ricini* (b) silk fibers, acquired with several different recycle delays in the quadrupole-echo pulse sequence.

The individual spectra have been scaled in order to reflect their relative intensities after 20 000 scans. It is seen that the line shapes become significantly distorted upon decreasing the recycle delay. This distortion is attributed to differences in the spin−lattice relaxation due to motions on different time scales, given that these ^{2}H NMR spectra arise from the superposition of several components as described below. We note, nevertheless, that Rice et al.[21] had pointed out that a two-pulse quadrupole echo sequence may give rise to an apparent

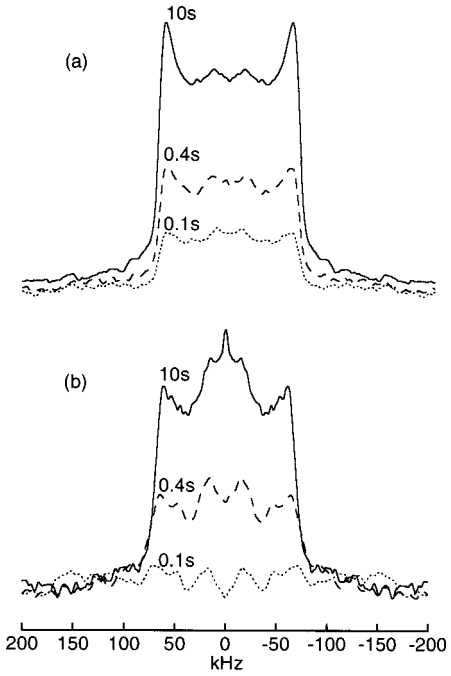

Figure 3. Experimental solid-state ^{2}H NMR spectra of [3′,5′-$^2H_2$]Tyr-labeled *B. mori* (a) and *S. c. ricini* (b) silk fibroin. Spectra were obtained with the quadrupole pulse sequence using repetition times of 10.0, 0.4, and 0.1 s, respectively. The spectra are plotted such that their intensities are directly comparable.

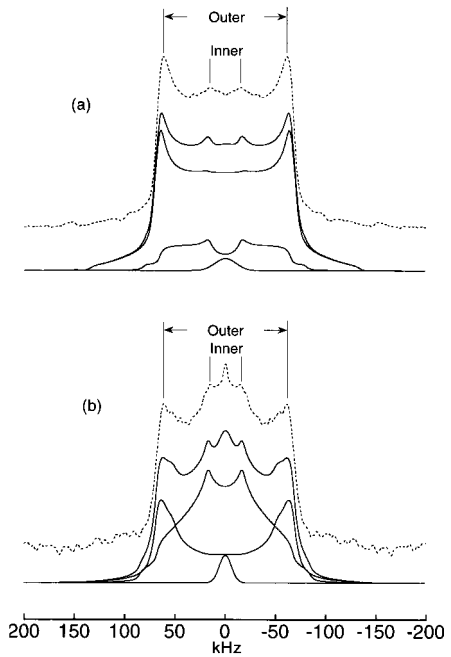

Figure 4. Experimental (dotted line) and calculated (solid line) solid-state ^{2}H NMR spectra of [3′,5′-$^2H_2$]Tyr-labeled *B. mori* and *S. c. ricini* silk fibroin. Spectra were obtained with the quadrupole echo pulse sequence with repetition times of 10 s, and simulation parameters are summarized in Table 1.

superposition of a rigid and a motionally averaged population, under conditions where a single jump rate applies that falls into the range of 10^4-10^6 Hz.

Figure 4 show the experimental (dotted line) and calculated (solid line) ^{2}H NMR spectra for *B. mori* (a) and *S. c. ricini* (b) silk fibroin, with a recycle delay of 10 s.

Because of their 2-fold symmetry, the phenolic side chains of Tyr can execute a π-flip motion about the $C_\beta-C_\gamma$ bond, between two orientations of equal energy. Generally, any molecular motion reduces the quadrupole coupling to a time-averaged value that is smaller than the rigid lattice constant. Thus, the small inner doublet with a splitting of 30 kHz, which is observed both for *B. mori* and *S. c. ricini* silk fibroin, is attributed to a fast π-flip motion of the phenolic ring. In contrast, the outer doublet with a splitting of 123 kHz corresponds to a slow motional component. The central peak at zero frequency is attributed to residual ^{2}HHO in the sample,[41] which can be taken into account in the lineshape simulation by a Gaussian function. The fraction of the ^{2}HHO component was assumed to be 0.8 and 2.5% of the total spectral intensity, for *B. mori* and *S. c. ricini*, respectively. A comparison of the two different kinds of silk fibroin in parts a and b shows that the line shapes differ significantly from one another, indicating that also the propensity for Tyr ring-flips must be different. Hence a simulation analysis was carried out with the MXQET program from Greenfield et al.,[38] assuming a two-site jump model and using the exchange rate and librational angle as variables. The line shapes could be consistently simulated with an asymmetry parameter of $\eta = 0.05$ and a quadrupole coupling constant of Qcc $=180.0$ kHz. At least two components were required to obtain a good fit, and these two components can be considered as rigid and as mobile on the deuterium NMR time scale. This dynamic interpretation is also supported by the changes in the spectral line shapes as a function of the recycle delay observed in Figure 3. The rates obtained from the simulation analysis are compiled in Table 1 for *B. mori* and *S. c. ricini* fibroin.

Table 1. Powder Pattern Simulation Results of ^{2}H Quadrupole-Echo Line Shapes for [3′,5′-$^2H_2$]Tyr-labeled *B. mori* and *S. c. ricini* Silk Fibroin

	B. mori			*S. c. ricini*		
component	rate (Hz)	libration (deg)	fract (%)	rate (Hz)	libration (deg)	fract (%)
fast	1×10^6	0	20	1×10^7	0	60
slow	1×10^3	10	80	1×10^4	20	40

The ^{2}H NMR spectrum of *B. mori* [3′ 5′-$^2H_2$]Tyr-labeled silk fibroin could be simulated best by assuming a fast motional component (10^6 Hz) that contributes 20% of the intensity and a slow motional component ($<10^3$ Hz) that contributes 80%. The respective proportions of the fast and slow populations were estimated by integrating the corresponding spectra.

A rotational jump of the phenolic ring is necessarily influenced by the degree of motional cooperativity with the surrounding groups, because the rotation of a bulky group must displace neighboring side chains to some extent. Hence the rate of a Tyr ring-flip can provide information about the conformational space around this particular side-chain. Since the repetitive regions of *B. mori* silk fibroin are supposedly packed in higher density, the dynamics of the Tyr side chain are expected to be restricted in this environment. Therefore, we attribute the slow and the fast motional components to residues in the repetitive and nonrepetitive regions, respectively. In fact, about 80% of all Tyr residues of *B. mori* silk fibroin occur within a (-Gly-Ala-Gly-Tyr-Gly-Ala-) sequence in the repetitive region. This fraction agrees quantitatively with the observed proportion of the slow motional component in Table 1. Moreover, ^{2}H NMR experiments have been performed for [3′, 5′-$^2H_2$]-Tyr-labeled silk fibers that were uniaxially aligned

either parallel or perpendicular to the external magnetic field (data not shown), and a slight dependence on the tilt angle was observed. These angle-dependent spectra confirm that there is indeed a preferred orientation of the Tyr ring in the ordered regions of the *B. mori* silk fiber.

Also in the case of *S. c. ricini* silk fibroin there is a slow and a fast motional component observed for the Tyr ring. Table 1 summarized the parameters obtained by simulating the corresponding ^{2}H NMR spectrum of Figure 4b. About 60% of the intensity arises from a fast motional component (10^7 Hz) and 40% from a slow one (10^4 Hz). As for *B. mori* silk fibroin, we attribute the two Tyr populations with different flip rates to regions with high and low packing densities. Since virtually all Tyr residues in *S. c. ricini* occur within Gly-rich sequences, this result demonstrates that the Gly-rich regions themselves must be differentially packed with high and low density. About 60% of the Tyr residues are comparatively mobile, and this proportion appears to correlate with a similar number of Tyr residues that are counted to be adjacent to three or more Gly residues. The remaining 40% of Tyr are located in regions of higher packing density. This dynamic information may be useful to predict the secondary structure of the Gly-rich domains in *S. c. ricini* silk fibroin. Recently, we have quantitatively analyzed the orientational distribution of Ala and Gly residues in *B. mori* cocoon silk[3] and in highly drawn *S. c. ricini* fibers.[41] It could be demonstrated that over 60% of all Gly moieties are oriented in both *B. mori* and *S. c. ricini*. However, the degree of alignment in *S. c. ricini* was significantly lower than in *B. mori*. Hence, the Gly-rich region of *S. c. ricini* silk fibroin is less well ordered than the repetitive region of *B. mori*. This reduced quality of alignment in the Gly-rich domain of *S. c. ricini* silk fibroin appears to correlate with the higher proportion of Tyr residues that can engage in fast π-flip motions.

Comparison with Other Crystalline Peptides. As described above, the molecular dynamics of aromatic side chains in solids have been extensively investigated by solid-state NMR, indicated that almost all of the rings are either rigid or undergo a π-flip motion at room temperature, depending on the crystal packing. Hiraoki et al. have investigated the phenyl ring dynamics of poly(L-phenylalanine) by ^{2}H NMR[27] and found that it is characterized by a fairly broad distribution of correlation times. The mean correlation time of this distribution was 1.2×10^6 Hz at 25 °C, which is close to that of the fast motional component of the *B. mori* and *S. c. ricini* silk fibroins. Likewise, the ring motion in crystalline *N*-acetyl-L-Asp-L-Pro-L-Tyr-*N*′-methylamide was found to be 1.1×10^6 Hz at 27 °C.[21] On the other hand, the Tyr ring flip in the pentapeptide [Leu^5] enkephalin was reported to be 5.6×10^4 Hz at 25 °C,[19] which is close to that of the slow motional component observed here for silk fibroin.

Conclusions

Solid-state NMR analysis was used to measure the side-chain dynamics of the tyrosine residues in silk fibroin from *B. mori* and *S. c. ricini*. The Tyr phenolic rings are found to be engaged in fast and slow π-flip motions, but with significantly different proportions in the two kinds of silk. In *B. mori* fibroin about 80% of all Tyr residues are motionally restricted and occur in regions with a high packing density. We suggest that their reduced mobility corresponds to a Gly-Ala repeat region. In the case of *S. c. ricini* silk fibroin, virtually all Tyr residues are located in Gly-rich domains, which give rise to both slow and fast motional components. Only about 40% of Tyr moieties are motionally restricted, while the remaining 60% occur in Gly-rich regions that are comparatively loosely packed.

Acknowledgment. The authers are grateful to Prof. Makoto Demura, Hokkaido University, for helpful discussions. T.A. acknowledges support from the Program for Promotion of Basic Research Activities for Innovative Biosciences, Japan, and a Grant-in-Aid for JSPS Fellows. A.S.U. thanks the DFG for supporting TP B13 in SFB 197.

References and Notes

(1) Asakura, T.; Kaplan, D. L. In *Encyclopedia of Agricultural Science*; Arutzen, C. J., Ed.; Academic Press: London, 1994; Vol. 4, pp 1−11.
(2) Mita, K.; Ichimura, S.; James, T. C. *J. Mol. Evol*. **1994**, *38*, 583.
(3) Demura, M.; Minami, M.; Asakura, T.; Cross, T. A. *J. Am. Chem. Soc*. **1998**, *120*, 1300.
(4) Asakura, T.; et al. To be submitted for publication.
(5) Kameda, T.; Ohkawa, Y.; Yoshizawa, K.; Naito, J.; Itoh, T.; Ulrich, A. S.; Asakura, T. *Macromolecules* **1999**, *32*, 7166.
(6) Asakura, T. *Bioindustry* **1987**, *4*, 36.
(7) Asakura, T.; Kanetake, J.; Demura, M. *Polym.-Plast. Manufact. J*. **1989**, *28*, 453.
(8) Asakura, T.; Murakami, T. *Macromolecules* **1985**, *18*, 2614.
(9) Asakura, T.; Kashiba, H.; Yoshimizu, M. *Macromolecules* **1988**, *21*, 644.
(10) Yukuhiro, Y.; et al., Personal communication.
(11) Mello, C. M.; Senecal, K.; Young, B.; Voudros, P.; Kaplan, D. In *Silk Polymers-Materials Science and Biothechnology*; Kaplan, D., Adams, W. W., Farmer, B., Viney, C., Eds.; ACS: Washington, DC, 1994; p 67.
(12) Ulrich, A. S.; Grage, S. L. In *Solid State NMR of Macromolecules*; Ando, I., Asakura, T., Eds.; 1998; pp 190−211.
(13) *Solid State NMR of Polymers*; Mathias, L. J., Ed.; Plenum Press: New York, 1991.
(14) Gall, C. M.; Diverdi, J. A.; Opella, S. J. *J. Am. Chem. Soc*. **1981**, *103*, 5039.
(15) Schaefer, J.; Stejstical, E. O.; Mckay, R. A. *J. Magn. Reson*. **1984**, *57*, 85.
(16) Frey, M. H.; DiVerdi, J. A.; Opella, S. J. *J. Am. Chem. Soc*. **1985**, *107*, 7311.
(17) Hiyama, Y.; Silverton, J. V.; Torchia, D. A.; Gerig, J. T.; Hammond, S. J. *J. Am. Chem. Soc*. **1986**, *108*, 2715.
(18) Saito, H.; Ishida, M.; Yokoi, M.; Asakura, T. *Macromolecules* **1990**, *23*, 83.
(19) Rice, D. M.; Wittebord, R. J.; Griffin, R. G.; Meirvitch, E.; Stimson, E. R.; Meinwald, Y. C.; Freed, J. H.; Scheraga, H. A. *J. Am. Chem. Soc*. **1981**, *103*, 7707.
(20) Frey, M. H.; Opella, S. J.; Rockwell, A. L.; Gierasch, L. M. *J. Am. Chem. Soc*. **1985**, *107*, 1946.
(21) Rice, D. M.; Meinwald, Y. C.; Shceraga, H. A.; Griffin, R. G. *J. Am. Chem. Soc*. **1987**, *109*, 1636.
(22) Naito, A.; Iizuka, T.; Tsuji, S.; Price, W. S.; Hayamizu, K.; Saito, H. *J. Mol. Struct*. **1995**, *355*, 55.
(23) Kitazawa, S.; Hiraoki, T.; Hamada, T.; Tsutumi, A. *Polym. J*. **1994**, *26*, 1213.
(24) Tsutsumi, A. *Prog. Polym. Sci*. **1993**, *18*, 651.
(25) Yamaguchi, M.; Tsutsumi, A. *Polym. J*. **1993**, *25*, 131.
(26) Yamaguchi, M.; Tsutsumi, A. *Polym. J*. **1993**, *25*, 427.
(27) Hiraoki, T.; Kogame, A.; Nishi, N.; Tsutsumi, A. *J. Mol. Struct*. **1998**, *441*, 243.
(28) Hiraoki, T.; Tomita, K.; Kogame, A.; Tsutsumi, A. *Polym. J*. **1994**, *26*, 766.
(29) Kitazawa, S.; Hiraoki, T.; Tsutsumi, A. *J. Mol. Struct*. **1995**, *355*, 87.
(30) Burke, P. A.; Griffin, R. G.; Klibanov, A. M. *Biotechnol. Bioeng*. **1993**, *42*, 87.
(31) Gall, C. M.; Cross, T. A.; DiVerdi, J. A.; Opella, S. J. *Proc. Natl. Acad. Sci. U.S.A*. **1989**, *79*, 101.
(32) Sparks, S. W.; Cole, H. B. R.; Torchia, D. A.; Young, P. E. *Chem. Scr*. **1989**, *29A*, 854.

(33) Leo, G. C.; Colnago, L. A.; Valentine, K. G.; Opella, S. J. *Biochemistry* **1987**, *26*, 854.
(34) Asakura, T.; Minami, M.; Shimada, R.; Demura, M.; Osanai, M.; Fujito, T.; Imanari, M.; Ulrich, A. S. *Macromolecules* **1997**, *30*, 2429.
(35) Ishida, M.; Asakura, T.; Yokoi, T.; Saito, H. *Macromolecules* **1990**, *23*, 88.
(36) Nicholson, L. K.; Asakura, T.; Demura, M.; Cross, T. A. *Biopolymers* **1993**, *33*, 847.
(37) *Nuclear Magnetic Resonance Probes of Molecular Dynamics*; Tycko, R., Ed.; Kluwer Academic Publishers: Dordrecht, The Netherlands, 1994; pp 27−106.
(38) Greenfield, M. S.; Ronemus, A. D.; Vold, R. L.; Vold, R. R.; Ellis, P. D.; Raidy, T. E. *J. Magn. Reson*. **1987**, *72*, 89.
(39) Asakura, T. *Makromol Chem*. **1981**, *182*, 1135.
(40) Asakura, T.; Watanabe, Y.; Itoh, T. *Macromolecules* **1984**, *17*, 2421.
(41) Asakura, T.; Demura, M.; Watanabe, Y.; Sato, K. *J. Polym. Sci.* **1992**, B, *30*, 693.
(42) Asakura, T.; Itoh, T.; Okudaira, M.; Kameda, T. *Macromolecules* **1999**, *32*, 4940.

MA991344G